International Conference on Estuaries and Coasts
November 9-11, 2003, Hangzhou, China

A THREE-DIMENSIONAL MODELING OF TIDAL CIRCULATION IN COASTAL ZONES WITH WETTING AND DRYING PROCESS

Qimiao LU
W.F. Baird & Associates, 627 Lyons Lane, Oakville, Ontario, Canada, L6J 5Z7,
E-mail: qlu@baird.com, Tel.: (905) 845 5385

Abstract: A three-dimensional numerical modeling of tidal circulation in coastal areas is developed and presented in this paper. To simplify the model formulation, a multi-layer vertical grid structure is applied to partition a three-dimensional model into several vertically integrated two-dimensional models. Spatially discretized finite elements are used to fit complicated geometry often existing in coastal areas. The explicit two-step Lax-Wendroff scheme is utilized for time marching. A wetting and drying process is added and applied in the model to simulate the flooding and ebbing processes in coastal areas with wide floodplains. The model is initially calibrated in a wind-driven flow numerical experiment. The computed velocity profiles show good agreement with the analytical solution. The real application of the model is performed in Rusi Bay, P. R. China. The modeled tidal elevations and flow velocities are compared with the observed data. The comparison indicates good agreement between the model results and the observed data.

Key words: Numerical Modeling, Three Dimensional, Hydrodynamics, Tidal Circulation, Finite Element Method, Wetting and Drying Process.

1. INTRODUCTION

Information on hydrodynamic conditions in coastal waters is essential for planning and monitoring of coastal construction activities, resource exploration, disposal of industrial and domestic waste water, dumping of dredged materials, etc. A poor prediction of these conditions may result in a drastic impact on the environment and even loss of lives. Improving our understanding of the hydrodynamic phenomena in the coastal region is necessary to better serve the rapid development of the coastal engineering and deteriorating coastal environment.

A numerical model constructed with proper governing equations can provide a realistic setting for simulating physical phenomena such as tidal circulation in coastal regions by using a finite element model. The more physical parameters and spatial dimensions are considered in the model, the more realistic the simulated outcome will be. However, for the example of the tidal circulation simulation, even with simplifications, considerable amount of computer memory and computational time is required to generate solutions for the hydrodynamic equations formulated by a fully three-dimensional finite element method. To be more efficient in obtaining the solutions, without sacrificing significant accuracy, a fully three-dimensional problem can be reduced to multiple two or one-dimensional problems by averaging in one or two directions.

The present 3D model for tidal circulation is based on Li and Zhan's (1993) multi-layer model. In the model, water body is divided into a number of layers in columns. In each layer, the governing equations are integrated in vertical direction to simplify the model formulation and the finite element discretization is applied. A detailed formulation of the 3D model for tidal circulation is described in this paper. A wetting and drying simulation is developed to

simulate the flooding and drying phenomena in wide floodplains which often exists in coastal regions. The model is verified in a wind driven flow numerical experiment and applied in Rusi Bay, P.R. China, to simulate the tidal circulation for the purpose of validation.

2. THE GOVERNING EQUATIONS

2.1 HYDRODYNAMIC EQUATIONS

With the assumption of hydrostatic pressure distribution, the governing equations describing the fluid motion are the continuity equation and momentum equations shown as follows:

$$\frac{\partial u_j}{\partial x_j} = 0 \tag{1}$$

$$\frac{\partial u_i}{\partial t} + u_j \frac{\partial u_i}{\partial x_j} + \delta_{ij} f u_j + \frac{1}{\rho}\frac{\partial P}{\partial x_i} = \frac{1}{\rho}\frac{\partial \tau_{ij}}{\partial x_j} \tag{2}$$

$$\frac{\partial P}{\partial x_3} - \rho g = 0 \tag{3}$$

$$(i = 1,2;\ \ j = 1,2,3;)$$

where u_i is the component of flow velocity in the x_i direction, respectively (see Fig.1), t is time, ρ is the density of water, P is the pressure, f is the Coriolis parameter, $f=2\Omega\sin\theta$, Ω is the angular frequency of the earth rotation ($\sec^{-1}$), θ is the latitude of the computed region (degree), τ_{ij} are the interfacial shear stresses, and $\delta_{ij} = \begin{bmatrix} 0 & -1 & 0 \\ 1 & 0 & 0 \end{bmatrix}$.

2.2 THE EQUATIONS IN MULTI-LAYER MODEL

This model adopts a multiple layer system in which the water column is divided into a number of layers as shown in Fig. 1. The variables in each layer are assumed to have small fluctuations or gradients in the vertical direction so simple averaging can be applied to obtain the first moment (the mean) of the variables. This can convert a fully three-dimensional problem into a set of multiple two dimensional problems without loosing much generality. Averaging the hydrodynamic equations in each layer can be achieved by integrating the equations in the vertical direction, e.g.

$$\overline{\beta} = \frac{1}{h^{(k)}} \int_{x_3^{(k)}}^{x_3^{(k+1)}} \beta \, \mathrm{d}\, x_3 \tag{4}$$

where $h^{(k)} = x_3^{(k+1)} - x_3^{(k)}$, is the thickness of the k-th layer, $x_3^{(k+1)}$ and $x_3^{(k)}$ are the altitudes at the upper and lower levels of the k-th layer, respectively.

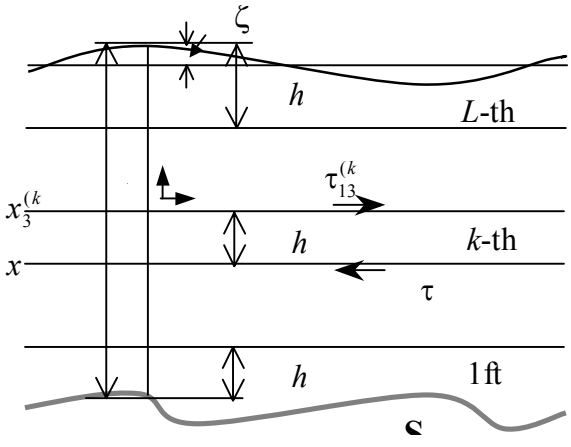

Fig. 1 Variable definition and layer arrangement in the multi-layer model

Considering the k-th layer in Fig. 1, the vertical integration of Eq. (3) resolves the differential equation and the pressure distribution becomes

$$P = P_0 + \sum_{i=k+1}^{L} \rho_i g h^{(i)} + \rho_k g\left(x_3^{(k+1)} - x_3\right) \qquad \left(x_3^{(k)} \le x_3 \le x_3^{(k+1)}\right) \tag{4}$$

where L is the total number of layers in the water column, ρ_i is the density of water in the i-th layer, and P_0 is the pressure at the water surface.

The vertically integrated form of the horizontal momentum equations, Eq. (2), for the k-th layer can be rewritten as follows

$$\frac{\partial U_i^{(k)}}{\partial t}+\frac{\partial}{\partial x_j}\left(\frac{U_i^{(k)}U_j^{(k)}}{h^{(k)}}\right)+u_i^{(k+1)}u_3^{(k+1)}-u_i^{(k)}u_3^{(k)}+\delta_{ij}fU_j^{(k)}$$
$$+\frac{h^{(k)}}{\rho^{(k)}}\frac{\partial}{\partial x}\left(P_0+\sum_{l=k+1}^{L}\rho^{(l)}gh^{(l)}+\rho^{(k)}\left(x_3^{(k+1}-x_3\right)\right) \tag{5}$$
$$-\frac{1}{\rho^{(k)}}\left[\left(\tau_{i3}^{(k+1)}-\tau_{i3}^{(k)}\right)+\rho^{(k)}\nu\frac{\partial^2 U_i^{(k)}}{\partial x_j\partial x_j}\right]$$

Here i, j=1, 2; the superscript (k) denotes the values of variables in the k-th layer; $U_i^{(k)}=\int_{x_3^{(k)}}^{x_3^{(k+1)}}u_i dx_3 \quad (i=1,2)$ is the discharge per unit width in the x_i-direction in the k-th layer; $\tau_{i3}^{(k)}$ is the averaged viscous stresses associated with the vertical coordinate, τ_{i3} $(i=1,2)$ in the k-th layer.

Using the conditions that the bottom vertical velocity is zero (impermeable bed condition) and the surface vertical velocity varies in time with the free surface elevation, the continuity equation, Eq. (1), after integration over water depth can be expressed as follows

$$\frac{\partial\zeta}{\partial t}+\sum_{l=1}^{L}\frac{\partial U_j^{(l)}}{\partial x_j}=0 \quad (j=1,2) \tag{6}$$

where ζ is water surface elevation as shown in Fig. 1. And for the intermediate level, one has

$$u_3^{(k)}=-\sum_{l=1}^{k-1}\frac{\partial U_j^{(l)}}{\partial x_j} \quad (j=1,\ 2) \tag{7}$$

Eq. (6) is used to determine water surface elevation, whereas Eq. (7) is the governing equation for solving the vertical velocity u_3.

2.3 BOUNDARY CONDITIONS

The existence, uniqueness, and of course the accuracy of the solutions of the above equations mentioned are heavily dependent on the boundary conditions that are prescribed. In tidal circulation flows, there are basically two types of boundaries. One is the close boundary or the land boundary and the other is the open boundary or the water boundary. On the open boundary, the velocities are generally specified at the water interface at each layer of the system or the water elevation is generally prescribed at the surface. The surface shear stresses such as the wind stresses are imposed at the interface between water and air. The surface shear stresses are neglected if the wind imposition is not considered. The no-slip and impermeable bed conditions are generally specified on the close boundary where water meets land and seabed.

In the tidal circulation model, the initial values are usually set as a constant for the initial spin up period.

3. FINITE ELEMENT FORMULATION

The unsteady nature of most of the coastal phenomena complicates finite element formulation of coastal problems, and the result is that enormous computational time is

required to obtain the finite-element solutions. Recently, this technique has gained popularity mainly because of the advances in high speed computing and particularly the use of parallel computational techniques capable of handling massive data "crunching" more efficiently and effectively. In fact, the finite element method is seen to be advantageous over the finite difference method especially in coastal problems where it offers great flexibility due to non-uniform boundary geometry. In this model, the finite element method with four-nodal elements is employed. The final linear system of algebraic equations is given as

$$\mathbf{A}\dot{\zeta} + \mathbf{R} = 0 \tag{8}$$

$$\mathbf{A}\dot{\mathbf{U}}_i^{(k)} + \mathbf{P}_i^{(k)} = 0 \qquad (i = 1,2) \tag{9}$$

$$\mathbf{A}\mathbf{u}_3^{(k)} = \mathbf{S}^{(k)} \tag{10}$$

Here **A** is a mass matrix; **P**, **R**, and **S** are known vectors; $\dot{\zeta}$ and $\dot{\mathbf{U}}$ are the temporal derivatives of surface elevation and velocities, respectively.

The system of algebraic equations, Eqs. (8) ~ (9), can be solved by employing an appropriate time marching scheme. This model employs the two-step finite difference Lax-Wendroff scheme. As result, the system at the first half step is given as

$$\begin{aligned} \mathbf{A}\mathbf{U}_i^{(k),n+1/2} &= \mathbf{A}\mathbf{U}_i^{(k),n} - \frac{\Delta t}{2}\mathbf{P}_i^{(k),n} \\ \mathbf{A}\zeta^{n+1/2} &= \mathbf{A}\zeta^{n} - \frac{\Delta t}{2}\mathbf{R}^{n} \end{aligned} \tag{11}$$

and at the second half step is written as

$$\begin{aligned} \mathbf{A}\mathbf{U}_i^{(k),n+1} &= \mathbf{A}\mathbf{U}_i^{(k),n} - \Delta t\mathbf{P}_i^{(k),n+1/2} \\ \mathbf{A}\zeta^{n+1} &= \mathbf{A}\zeta^{n} - \Delta t\mathbf{R}^{n+1/2} \end{aligned} \tag{12}$$

Since the finite element formulated equations, Eqs. (11), (12) and (10), consist of the coefficient mass matrices, the inverse of the coefficient matrix is necessary to simultaneously evaluate the unknowns in the next time step. This requires more computational time and storage. For the present study, the finite element formulated equations can be solved by using a lumped mass technique (Kawahara et al., 1982) which has been proven very powerful and numerically stable in other dynamic problems. Lumping mass technique distributes the mass of an element to the points of its four nodes equally to diagonalize the coefficient matrix. The lumping technique can save about 50% in computer storage and avoid the inversion of the coefficient matrix (**A**).

4. WETTING AND DRYING PROCESS

Wide floodplains often exist in coastal areas. The floodplains are usually dried at low water and wetted at high water in a tidal cycle. Though the kinetic energy of the flows in floodplains is small and often neglected in the hydrodynamic computations, the storage of water in wide floodplains can considerably affect the tidal flows in deep channels. For instance, the floodwater coming from outer sea fills the shallow floodplains during flood periods and diverse the main flow in the deep channel. On the other hand, the stored water in the floodplains converges into the deep channels during ebb periods resulting in strengthening the main flows. If no wetting and drying process is employed in this situation, the numerical model may not accurately describe the tidal circulation in both deep channels and floodplains. Therefore, it is necessary to develop the wetting and drying process routines in the 3D model to expand the model adaptability in coastal areas with wide floodplains.

In the wetting and drying process, water level is usually used to determine whether a grid is dry or wet. If the water level is higher than the bed altitude at a grid, the grid is assumed to be wet and then it is included in the computations. Otherwise, the grid is assumed to be dry and it

is withdrawn from computations. This concept is based on the physical flooding phenomena and obviously applicable to an ebb period. However, for flooding processes, it raises a problem how to determine the water level at a grid which has already been dry and excluded in the computations. The water level in these dried grids is undefined. For this reason, "virtual water level (VWL)" which does not exist in practice is introduced. The VWL at a dry grid is calculated by using a typical function in the computations of tidal elevation. The detailed calculations for VWL are described in the following section.

After knowing VWL, virtual water depth (VWD) can be calculated as the difference of the VWL and the bed altitude. The VWD is used to identify the dried situation, whether a grid is wet or dry. Theoretically, a grid is dry if VWD is less than zero. Otherwise, a grid is wet. However, this criterion will induce large numerical errors and even cause the computations unstable when the VWD becomes zero or very small since the bottom friction is inversely proportional to the water depth. So small water volume should be kept at a dried grid to achieve the stable computations and reduce numerical errors. Thus, a grid is wet when the VWD is larger than the "minimum water depth" (MWD) otherwise it is dry. The MWD should be set a proper constant value. Using a large value for the MWD induces the mass conservation problem while using a small value causes computations unstable. Experience from previous simulations indicates that the MWD set from 0.1m to 0.3m can avoid the numerical instability and the computational errors. In this situation, the kinetic energy of such small residual water at a dry grid can be neglected without losing the computational accuracy.

Now the key issue in the drying up technique is how to determine the VWD or VWL. Evidently, the VWL at a wet grid is set as the water level computed from the continuity equation. However, it becomes undefined if a grid is dry. In the natural flooding phenomena, a dry grid is firstly flooded by the water body coming from adjacent grids that are already wet. So the following expression is suggested to calculate the VWL at a dry grid.

$$\zeta_{v,i} = \max(\zeta_{i,1}, \zeta_{i,2}, \cdots, \zeta_{i,J}) \tag{13}$$

where $\zeta_{v,i}$ is the VWL at a dry grid i; $\zeta_{i,j}\,(j=1,\cdots,J)$ is the known VWL at the adjacent grids around the grid i; J is the number of the adjacent grids. However, Eq. (13) becomes still undefined if all adjacent grids are dry. To avoid this problem, the following procedure for calculating the VWL at a dry grid is suggested.

Ⅰ. Assign the dry status as one for dry grids and zero for wet grids according to the water depth computed in previous step.

Ⅱ. Set the calculating sequences from the deepest grid to the shallowest grid according to the bed altitudes.

Ⅲ. Compute VWL using Eq. (13) and assign the dry status as zero at the grid.

Ⅳ. Repeat step III until the VWLs at all dry grids are updated.

The above calculation procedure also reveals the physical processes of flooding. That is, the lowland of floodplains is flooded firstly and then followed by the highland. The VWD can be obtained from the following formula

$$H_v = \zeta_v + h \tag{14}$$

Here, H_v is VWD. Thus, the dry status for the next step can be determined according to VWD and

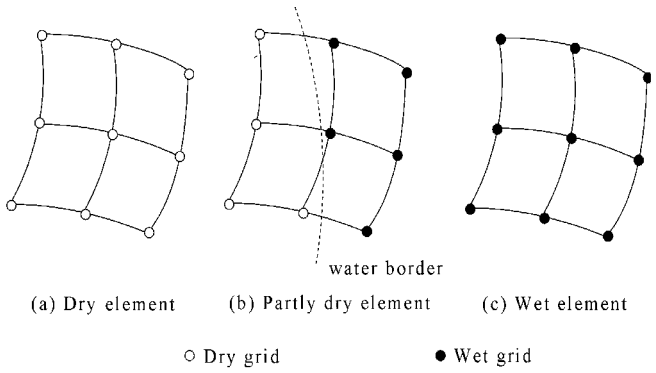

Fig. 2 Three types of finite elements in wetting and drying process

MWD. That is, a grid is dry if $H_v \le MWD$ and a grid is wet if $H_v > NWD$.

There are three dry types for finite elements --- dry, partly dry and wet elements (see Fig. 2). For dry elements, the finite element integration of the given equations becomes zero due to the absence of kinetic energy in dry elements. For wet elements, the normal integration as described in Section 3 is applied. For partly dry elements, the integration of momentum equations is neglected because the kinetic energy in such shallow water body is very small. Therefore, flow velocities at the dry grids are set at zero. However, the integration of continuity equation in the partly dry elements is calculated in order to maintain the mass conservation. The integration is only performed in the wet part of the partly dry elements. In the computations of tidal elevation, Eq. (13) is used instead to calculate the VWLs at dry grids.

5. MODEL VERIFICATION

A simple test case will be carried out for the first step of verifying the numerical model. Consider a closed uniform rectangular basin 2 km long and 0.8 km wide with water depth h=10m. The free surface is subjected to a constant uniform stress $\tau_{13}^{(L+1)} = 0.15$ (Nm^{-2}). The water body is divided into 40 rectangular elements horizontally and 11 equal layers vertically. To illustrate the vertical circular flow pattern subjected to the boundary conditions as prescribed above, the mesh near the close boundaries is refined to account for the larger spatial variations near the walls (see Fig.3). The no-slip boundary conditions are employed around the vertical walls as well as at the basin bed. Other parameters are set as: Δt=5s, ν=0, f=0, and ρ=1000kg/m^3. The surface setup and setdown at the basin ends caused by the prescribed forcing and boundary conditions is only in the order of 10^{-2}m.

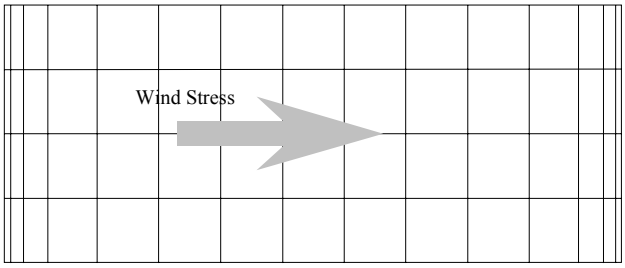

Fig. 3 Grid distribution in the driven flow test case

The computed horizontal velocity profile in steady state at the center of the rectangular basin is plotted with the corresponding analytical solutions in Fig. 4. The vertical eddy viscosity, ε, used in the test case is equal to 0.01m^2/s. It can be seen that the computed profile agrees quite well with the analytical solution.

The simulated velocity vectors in the side view are shown in Fig. 5. The figure shows no residual current near the basin edges and the velocity vectors are basically vertical near the walls. This is consistent with the ideal flow pattern for steady and uniform surface stress with insignificant setup and setdown. Fig. 5 also reveals that the velocity magnitude tends to zero at the upper water column in the central basin and this can also be observed in Fig. 4 where the horizontal velocity profile changes its direction having zero crossing point at the level corresponding to -3.8 m.

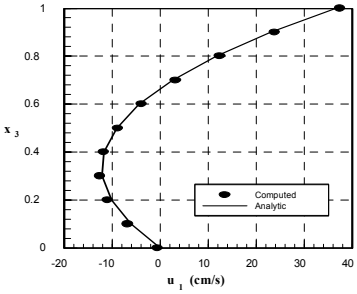

Fig. 4 The comparison of the computed velocity profile with analytical solution

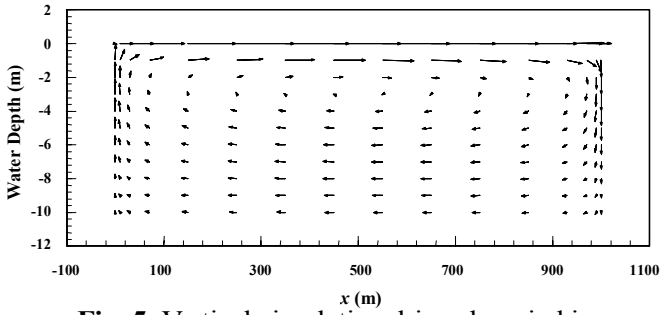

Fig. 5 Vertical circulation driven by wind in a rectangle basin

6. APPLICATION TO RUSI BAY

To extend the adaptability of the three-dimensional model to coastal settings and verify the wetting and drying process, the model was applied to Rusi Bay during a spring tide period when the tidal fluctuation attains its extreme. Rusi Bay is located in Jiangsu Province, China, just north of Yangtze River (at latitude 32.2°N and longitude 120.3°E, see Fig. 6). The Bay has a surface area of about 1080 km^2 with a west-eastern length of 53 km and a mouth width of 28 km. There is a deep waterway, called Xiao Miao Hong channel, in the central of the Bay. The channel is partitioned into three branches, namely north, middle and south branches, by the two submerged bed dunes over the mouth of the Bay. There are two wide floodplains beside the channel. The bed height of the floodplains is over the mean lowest water level so the floodplains often dry up at low water level and flood at high water level. About 40% of the area of the Bay will dry up at the lowest water level. Therefore, it is necessary to apply the drying up technique in the model to achieve accurate simulations.

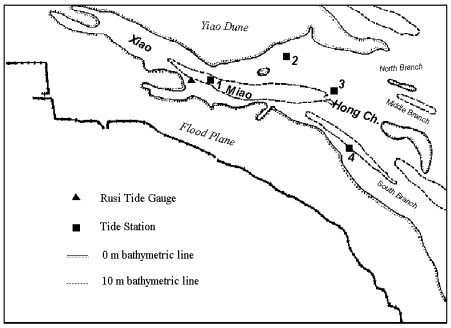

Fig. 6 Bathymetry and location of the tide stations in Rusi Bay

The tidal fluctuation in the Bay is very large. The historically recorded maximum tidal range, which is the difference of the highest tidal elevation and the lowest tidal elevation in a tidal period, reaches about 9m. The averaged tidal range in spring tides is about 4.3m while the annual mean tidal range is about 2.7m. Such large tidal range can induce very strong tidal currents in the Bay. The maximum flow velocity was measured to be more than 2m/s. The big tidal water storage in the floodplains changes the characteristics of tidal circulation in the Bay because the stored water should pass through the narrow deep channel during flood and ebb periods. It is difficult to simulate such strong tidal flows in such complicated area with wide floodplains.

The field data available for the model calibration are shown in Fig. 6. These field data are applied to verify this model. The grids were generated using the Grid Generator software (Lu and Wai, 1994). The vertical water column was divided into 5 layers in the entire area. The number of layers used in the water column is dependent on the water depth such that the number of elements used in each layer relates to the area of each horizontal plane. The grid parameters in the five layers are listed in Table 1. As the plane area decreases in the downward direction, the numbers of nodes and elements decrease from the surface layer to the bottom layer. The thickness of interior layers is held constant, while the thickness of bottom layer is altered with the seafloor topography and the surface layer is varied with tidal elevations. Fig. 7 shows the four nodal quadrilateral finite elements in the surface layer.

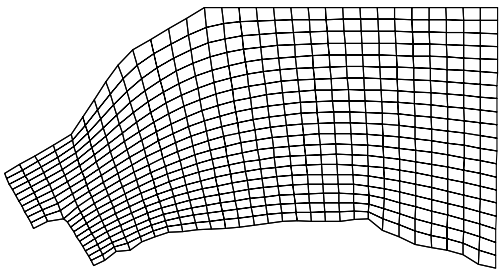

Fig. 7 Grid distribution of the surface layer in Rusi bay

The simulation period is based on the spring tide in Sept. 11, 1992. The tidal elevations used in the previous 2D model (Lu, 1993) for boundary conditions are also employed to control the open boundary in the present application.

Table 1 Elevation, thickness, numbers of nodes and elements in each layer

Layer	Elevation at top level (m)	Elevation at bottom level (m)	Thickness Of the layer (m)	Number of nodes	Number of elements
5	Surface	-3.	Varied with surface elevation	631	580
4	-3.	-6.	3.	410	347
3	-6.	-9.	3.	334	276
2	-9.	-12.	3.	262	203
1	-12.	Seabed	Varied with water depth	179	116
Total				1816	1522

The tidal elevations and flow velocities computed by the 3D model are compared with the measured values. The computed tidal elevations agree quite well with the observations at the tidal gauge (Fig. 8). The velocity profiles computed by the model are compared with the measurements at the four stations in the time interval of an hour (Fig. 9). The figure shows that the computed velocities agree well with the observations in both time series and vertical distribution. The mean relative error for tidal elevation is 2% while the mean relative error for flow velocities is under 9% for the four stations. The maximum error of 26% for velocities is found in the second ebb period at Station 1#, which may result from the coarse grids used in the model that cannot accurately describe the sharp topography of seabed in this area. As the result, the simulated tidal circulation generally depicts the physical flow pattern in Rusi Bay.

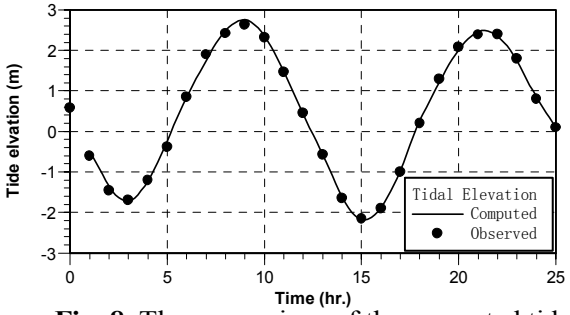

Fig. 8 The comparison of the computed tidal elevation with the measurement at the gauge

To illustrate the tidal flooding and ebbing processes simulated by using the developed wetting and drying process, the flow velocity vectors on the surface layer in the flood and ebb periods are plotted in Fig. 10. Fig. 10a shows the flooding (wetting) process at the mean water level when the lowlands of floodplains are being flooded. The flow vectors on the floodplains drift off the channel. This depicts the natural flood flow patterns on the floodplains and may not be described by the models without wetting and drying process capability. Fig. 10b shows that most of floodplains are wet and the flow velocities reach maximum after one-hour lapse. The ebb

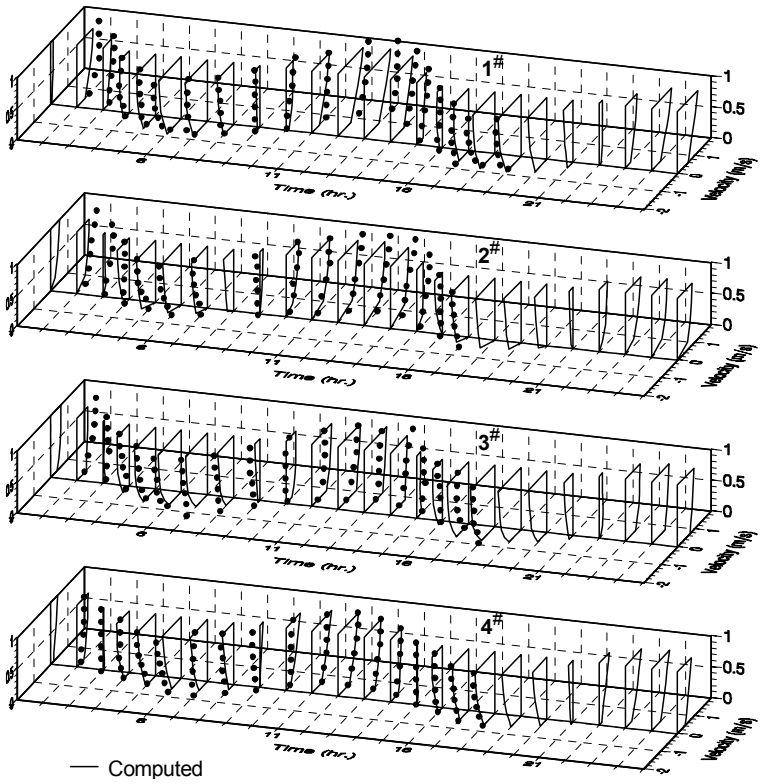

Fig. 9 The verification of velocity profiles in time series in Rusi bay application

flow vectors at the mean water level are shown in Fig. 10c, in which the dry highland of floodplain is observed. The ebb flow vectors on the floodplains are shifted to the deep channel. The flow pattern at low water level is shown in Fig. 10d. All floodplains are dry and the flows converge into the deep channel. These pictures depict the natural wetting and drying processes clearly.

7. CONCLUSIONS

A 3D finite element model for tidal circulation has been developed in coastal waters where water depths are considered shallow. Using multi-layer system in water columns and vertically averaging governing equations in each layer can reduce the degree of complexity of a full 3D finite element model but without losing much generality. This simplifies three-dimensional structure of the model and makes the model efficient.

A wetting and drying process was developed and applied in the 3D model to simulate tidal circulation on wide floodplains. Using the concept of virtual water level, the dry status for a grid is easily determined. A typical function and the sequence of calculation are suggested to compute the virtual water level at a dry grid. The minimum water depth introduced in wetting and drying process guarantees the computational stability without losing significant numerical accuracy. The values for the minimum water depth are proposed from 0.1m to 0.3m. Too large or too small values used for the minimum water depth may lead to numerical instability and large errors.

A preliminary test case was carried out by subjecting the model to a constant uniform surface stress on a rectangular basin. The results computed by the model correlated well with the analytical results. The model was also applied to Rusi Bay to simulate the tidal circulation during a spring tide period. The comparisons of the simulated results with the measurements show that the model can simulate with reasonable accuracy the characteristics of tidal circulation, such as tidal level fluctuation and velocity profiles. With this wetting and drying process function, the model is able to simulate natural flooding and

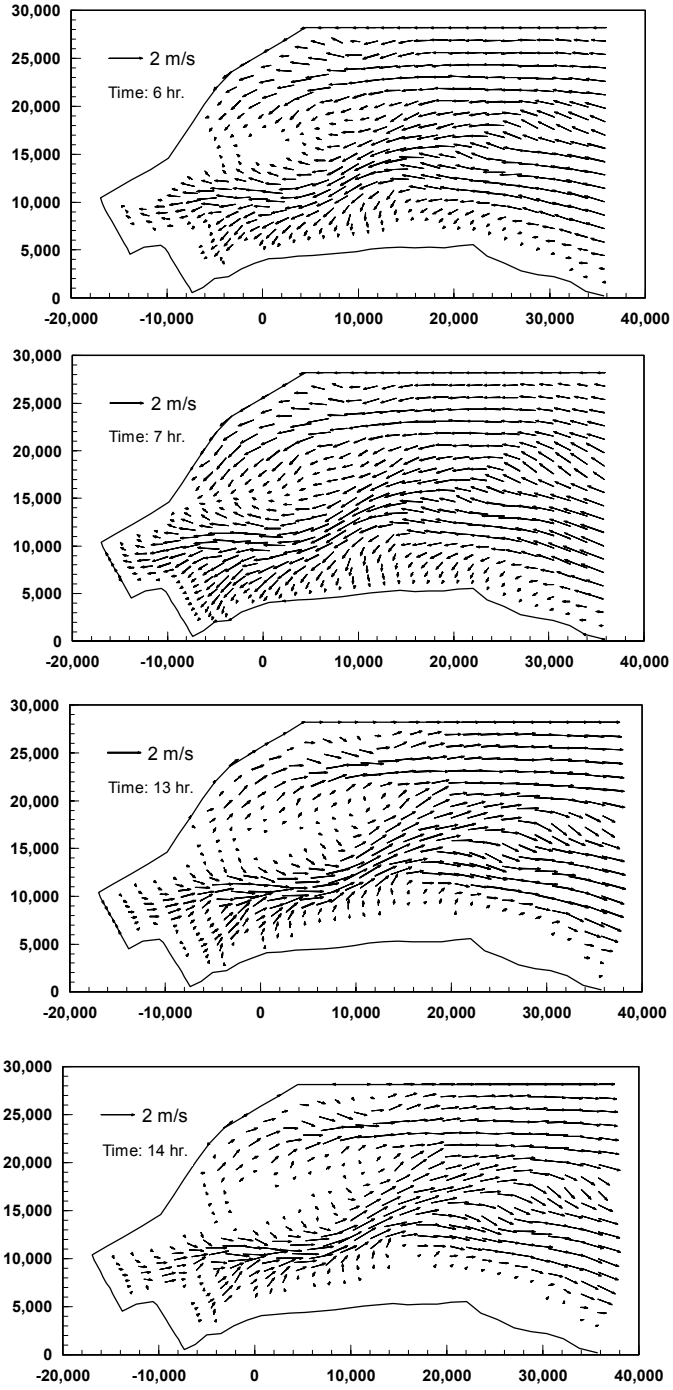

Fig. 10 The flow patterns at: a) flood mean water; b) high water; c) ebb mean water; and d) low water

ebbing processes in the Bay. To test the limitations and predictive capabilities of the model it is necessary to carry out more applications in the future.

REFERENCES

Kawahara, M., M. Kobayashi and K. Nakata (1982). "A three dimensional multiple level finite element method considering variable water density", in R. H. Gallagher, D. H. Norrie, J. T. Oden and O. C. Zienkiewicz (eds.), *Finite Element in Fluids,* Vol. 4, Wiley, Chichester, pp. 129-156.

Li, Y. S. and J. M. Zhan (1993). "An efficient three-dimensional semi-implicit finite element scheme for simulation of free surface flows", *Int. J. Num. Methods Fluids*, 16, 187-198.

Lu, Q.M. (1993). "Two-dimensional simulation for predicting the changes of tidal currents induced by the coastal engineering in Xiao Miao Hong waterway", *NHRI Technical Report*, Nanjing, China.

Lu, Q.M. and Onyx W.H. Wai (1994). "Numerical Grid Generation for Two or Three-Dimensional Mathematical Flow Model", *HKPolyU Technical Report*, Hong Kong